Microplastic and microfiber fluxes in the Seine River: Flood events versus dry periods

Robin Treilles, Johnny Gasperi, Romain Tramoy, Rachid Dris, Anaïs Gallard, Chandirane Partibane, Bruno Tassin

Microplastic and microfiber fluxes in the Seine River: Flood events versus Dry periods

TREILLES Robin[1*], GASPERI Johnny[2], TRAMOY Romain[1], DRIS Rachid[1], GALLARD Anaïs[1], PARTIBANE Chandirane[1], TASSIN Bruno[1]

[1] Leesu, Ecole des Ponts, Univ Paris Est Creteil, Marne-la-Vallee, France

[2] GERS-LEE Université Gustave Eiffel, IFSTTAR, F-44344 Bouguenais, France

*Corresponding author: robin.treilles@enpc.fr

Abstract

Studies on the influence of hydrodynamic conditions on anthropogenic microfiber (MF) and microplastic (MP) distributions in freshwater environments are sparse. In this study, we studied the influence of urbanisation gradient on the spatial variability of MFs and MPs. Temporal variability was also assessed by comparing the concentrations and fluxes of MFs and MPs under low flow conditions with those during the January-February 2018 flood event. For each period, Seine river water was collected upstream and downstream of Greater Paris and filtered through an 80 µm net at three different sampling sites. MFs were counted using a stereomicroscope, while MPs were analysed using micro-Fourier transform infrared spectroscopy coupled with siMPle analysis software. The highest concentrations of MFs and MPs were reported at the furthest downstream sites during both periods. However, high water flowrates and urbanisation gradient did not significantly impact MF and MP concentrations, sizes, or polymer distributions. The median MF and MP concentrations were 2.6 and 15.5 items/L and their interquartile ranges were 1.6 and 4.9 items/L (n=10),

respectively, illustrating relatively stable concentrations in spite of the urbanisation gradient and variations in the flowrate. In contrast to the concentration, size, and polymer distribution characteristics, MP mass fluxes were strongly affected by river flow. MF and MP fluxes show increases in the number and mass of particles from upstream to downstream. The downstream site presents high MP mass fluxes, which range between 924 and 1675 tonnes/year. These results may indicate significant MP inputs from the Paris Megacity through wastewater treatment plant effluents and untreated stormwater. The January-February 2018 flood event, which represented 14.5% of the year (in terms of time), contributed 40% of the yearly MP mass fluxes. Thus, flood events contribute strongly to MP fluxes.

KEYWORDS: microplastic, microfiber, microlitter, plastic pollution, flood, hydrological conditions

Graphical abstract

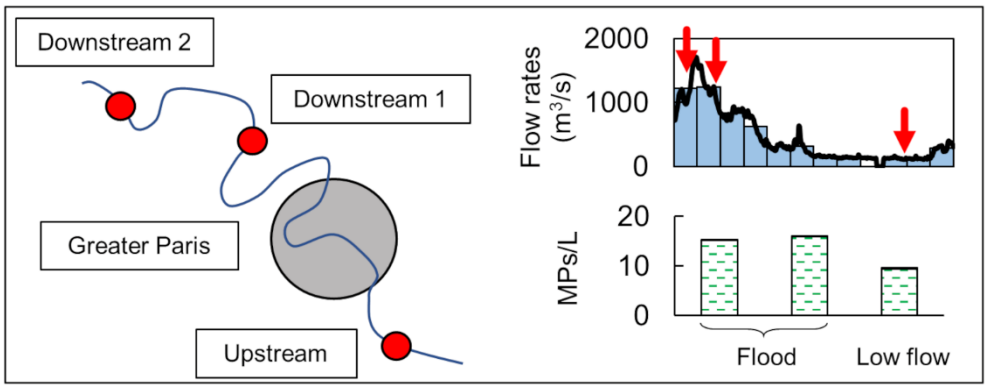

1. Introduction

Microlitter, such as microfibers (MFs) and microplastics (MPs), represent a threat to marine (Cole et al., 2011; Gall and Thompson, 2015; Jamieson A. J. et al., 2019) and freshwater environments (Blettler et al., 2017). An increasing number of studies have investigated the transport of microlitter in freshwater environments. The development of microlitter analysis in environmental matrices such as surface waters (Horton et al., 2017) and sediments (Klein et al., 2015) has led to significant advances in assessing the concentration of these particles.

However, very few studies have been conducted on the influence of hydrological conditions and urbanisation gradients on microlitter concentrations in rivers.

Several studies have observed higher concentrations of microlitter during low-flow periods than in high-flow conditions (de Carvalho et al., 2021; Rodrigues et al., 2018; Watkins et al., 2019; Wu et al., 2020). This difference in concentrations was attributed to a dilution effect. Other studies did not observe significant differences in microlitter concentrations between low and high-flow conditions (Schmidt et al., 2018; Wagner et al., 2019). According to these studies, other parameters may influence the microlitter concentrations. Several studies did not evaluate variation linked to flowrate seasonality, but focused on the impact of rain events during low-flow conditions. Hitchcock (2020) showed that under low-flow conditions, the MP concentration of a small urban estuary river increased during two days of heavy rain, from 400 particles/m^3 to 17 000 particles/m^3. Wong et al. (2020) observed a correlation between MP concentrations and precipitation in freshwater environments and noted a strong impact of runoff on MP distribution. Rain events may increase the MP input in rivers owing to the leaching of soil and sealed surfaces. Rain events can lead to combined sewer overflows and untreated stormwater discharge to rivers (Blettler et al., 2017). Thus, rain events may induce a flushing effect, that is, an increase in the MP input to freshwater resulting from mismanaged urban water (Schmidt et al., 2018). Other studies have suggested that there is no simple correlation between river flow and MP concentration (Kataoka et al., 2019; Wagner et al., 2019). Kataoka et al. (2019) observed a correlation between MP concentrations and water quality, but no relationship between MP concentrations and flowrates. Other studies have shown that flood events may play a key role in plastic debris loads in rivers (Roebroek et al., 2021; Tramoy et al., 2020b). Veerasingam et al. (2016) observed a significant increase in MP pellet concentrations in beach sediments after a flood event. These pellets may have been remobilised and more easily migrated from land to sea. Hurley et al. (2018) showed that a significant amount of the MP load stored in channel-bed sediments was exported after a flood. According to these studies, MPs may be efficiently

flushed from the river to the sea during a flood. Anthropogenic MFs are rarely considered in these studies, even though they are ubiquitous contaminants (Zhao et al., 2016). Thus, the relationship between microlitter concentration, flow rates, and precipitation is still debated.

Several studies concerning the influence of the urbanisation gradient have observed higher MP concentrations in urbanised, densely populated, and downstream areas (Kataoka et al., 2019; Schmidt et al., 2018; Wagner et al., 2019; Wu et al., 2020). In several of these studies, MP concentrations were correlated with population density (Kataoka et al., 2019; Wu et al., 2020). According to Wagner et al. (2019), plastic concentrations may be constant in rural areas but increase linearly in urban areas owing to inputs associated with urban discharge during rainy weather. Rodrigues et al. (2018) observed higher concentrations upstream of the catchment studied. This observation may be a particular to the sampling site, as the upstream part of the catchment studied has a higher population density (Rodrigues et al., 2018). However, Wong et al. (2020) observed no correlation between MP concentrations and population density. Thus, various conclusions may be drawn, depending on the sampling site.

In this study, MF and MP concentrations were estimated at three different sampling sites upstream and downstream from Greater Paris during low flow conditions, as well as during a flood event that occurred in January-February 2018. The main objectives of this work were to evaluate the influence of the urbanisation gradient and different hydrological conditions on the MF and MP concentrations and fluxes.

2. Materials and methods

2.1. Sampling sites

Three sampling sites were selected: (i) the first site, noted “Upstream”, is located 100 km upstream of Paris (Greater Paris, 8.9 million capita, 2 546 km^2, 3 700 cap/km^2) and downstream of the moderately dense city of Troyes (Troyes Champagne Metropolis, 170 167 capita, 889 km^2, 191 cap/km^2, with a waste water treatment plant capacity of 260

000 population equivalent) ; (ii) the two other sites are located 20 and 45 km downstream of Paris and noted as “Downstream 1” and “Downstream 2”, respectively. Upstream is less impacted by industrial activities, whereas Downstream 1 and 2 correspond to a dense urbanised area. Downstream 1 is located downstream from three significant waste water treatment plants (noted as WWTP, “Seine Centre”, “Seine Amont” and “Marne Aval”, which have treatment capacities of 240 000, 600 000 and 75 000 m^3 per day, respectively), Downstream 2 is located downstream of the most significant WWTP of Paris Megacity (Seine Aval, which has a treatment capacity of 1 700 000 m^3 per day, according to the Parisian Public Sanitation Authority) and is also located downstream of the confluence between the Seine River and Oise River, which is one of its main tributaries (Figure 1). The major potential sources of microplastics are: (i) Combined Sewer Overflows (CSO) of Greater Paris, (ii) Waste Water Treatment Plants (treatment capacity > 75 000 m^3 per day), (iii) untreated stormwater, and (iv) densely populated areas with intense industrial activities near the different sampling sites.

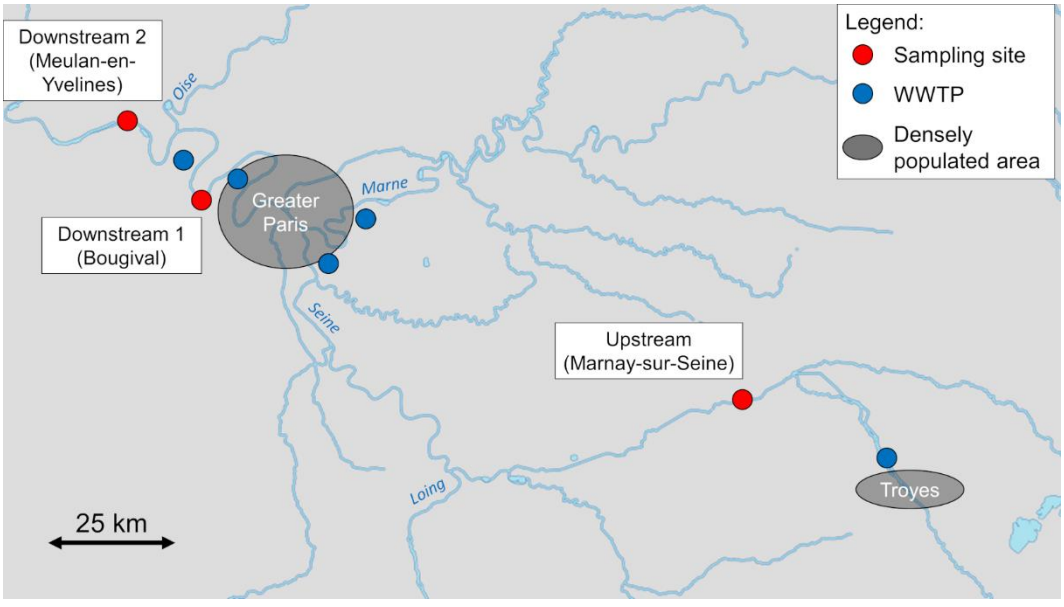

Figure 1: Location of the sampling sites, most significant Wastewater Treatment Plants (WWTPs, treatment capacity > 75 000 m^3 per day) and densely populated areas (the hydrographic network is from Geoportail France).

2.2. Sampling method

Three sampling campaigns were performed during contrasting hydrological conditions: two campaigns were conducted during the flood event that occurred in January-February 2018, represented by the numbers 1 and 2 in Figure 2 (01/26/18 and 02/21/18, $Q_{max\ Paris}$ = 1710 m^3/s, with a 10 year return period of Q_{10} = 1650 m^3/s and a 100 year return period of Q_{100} = 2400 m^3/s) and one campaign was conducted during the dry season during a low water level period, represented by the number 3 in Figure 2 (07/17/18, Q_{Paris} = 155 m^3/s). The Seine River was monitored by a surveillance network that followed the flow variations (Figure 2). Samples were collected at each site during the same day in the following order: Upstream, Downstream 1, and Downstream 2. One extra sample was collected on 02/21/18 from the Upstream sampling site (2 bis, green arrow in Figure 2). The first campaign (01/26/18) corresponded to a period of increasing flow just before the flow peak. The following campaign in February 2018 corresponded to a decrease in the water flowrate. The daily flowrates and water levels of each sampling campaign are presented in the supplementary data (Table S1). Between 20 and 30 L of water were manually collected from the bridges using a metal bucket and filtered through an 80 µm net. Plastic materials were banned to avoid any on-site contamination. The net was systematically rinsed before and after sampling. The samples were then stored in glass containers in a cold room (4°C).

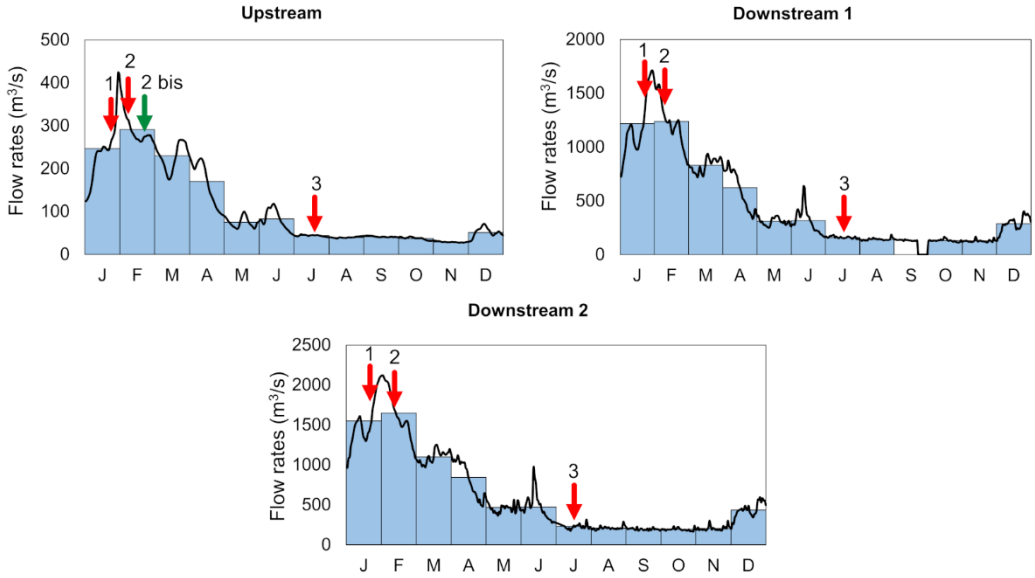

135

136 Figure 2: Daily flowrates (black lines) and monthly mean flowrate (blue bars) of the different
137 sampling sites for 2018. Date of sampling is represented by the red arrows (data from
138 http://hydro.eaufrance.fr, Upstream, Downstream 1 and Downstream 2 flowrates were
139 assessed using Pont-sur-Seine, Austerlitz and Vernon measurements, respectively). The
140 green arrow indicate the extra sample collected at the Upstream sampling site.

141 2.3. Analytical procedure

142 Samples were sieved using a 5 mm and a 1 mm sieve and separated into the 1-5 mm
143 fraction and <1 mm fraction. Sieving did not prevent the entrance of long fibers (> 5 mm) in
144 the <1 mm fraction, owing to their small diametres. Particles in the 1-5 mm fractions were
145 inspected under a stereomicroscope. Based on their colour, shape, and texture, suspected
146 plastic particles were set aside and characterised using infrared spectroscopy with
147 attenuated total reflectance (ATR-FTIR, Thermo ScientificTM iD7 accessory). This method is
148 based on Dris et al., 2017. For the <1 mm fraction, organic matter was oxidised using 30
149 wt% H_2O_2 digestion at 40°C for 48 h with 50 mL of solution and magnetic stirring (300 rpm).
150 Digestion was conducted at temperatures ≤ 40°C to avoid thermal degradation of the MFs
151 (Treilles et al., 2020). The solution was filtered through a metallic filter (Ø = 90 mm, porosity
152 = 14 µm). MP particles were then separated from mineral matter by densimetric separation

in a NaI solution ($\rho \geq 1.6$ g.cm^{-3}) in a separating funnel. The supernatant was filtered using the same metallic filters and the microlitter was characterised.

Because of their shapes, the automatization of MF detection with µFTIR and processing software cannot be implemented confidently. Indeed, confusions between MFs and MP fragments were frequently observed with automated µFTIR detection. For this reason, all MFs were manually counted under a stereomicroscope (Leica MZ12, with a size detection limit of 50 µm) coupled with an image analysis software (Histolab) according to the method developed by Dris et al. (2018), while MPs were counted and chemically characterized by µFTIR imaging, with no shape distinction. MFs are all anthropogenic fibers, including synthetic and non-synthetic fibers. This results in possible crossed data between MFs and MPs. However, we decided to keep the data in this form, as the size distribution between MPs and MFs is significantly different (Figure 5). Indeed, most of MPs are below 250 µm whereas MFs are above 1000 µm (Figure 5). This overlap of data may thus be negligible.

Once the MFs were counted, metallic filters were plunged in a crystallizer with 20 mL of filtered water and the particles were removed using an ultrasonic bath for 30 s. The filtered water was then poured into a 100 mL glass bottle. This resuspension step was repeated three times. Then, the metallic filter was rinsed one last time with 40 mL of filtered water. The glass bottle was vigorously stirred for 1 min to homogenise the content. Then, 10 to 20 mL of this volume, *i.e.,* 10 to 20 %, was filtered onto a Whatman® anodisc inorganic filter membrane (porosity: 0.2 µm, Ø 25 mm, with a filtration surface of Ø 14 mm).

The anodisc filters were analysed with Fourier transform infrared spectroscopy coupled with a microscope, using the Thermo Scientific Nicolet™ iN10 µFTIR in transmission mode. A Thermo Scientific® MCT/A Cooled Imaging detector with a spectral range of 4000 to 1200 cm^{-1} was used to avoid interference with the anodisc filter. An autobaseline correction was applied to all spectra. After the spectral background was defined, the mapping analysis mode was used on one scan. All particles on three 6 × 6 mm infrared maps were analysed, corresponding to 70% of the filtration surface of the filter. An atmospheric suppression correction was applied to all spectra. Maps were analysed using the siMPle analysis

181 software developed by Aalborg University, Denmark and the Alfred Wegener Institute,
182 Germany (Liu et al., 2019).
183 This method has a size detection limit of 25 µm. Each spectrum identified as a plastic
184 polymer by the siMPle software was checked by an operator for false positives. Particular
185 attention was paid to PE spectra, as false positives of these particles have been observed in
186 other studies (Witzig et al., 2020). siMPle assesses the number of particles and estimates an
187 order of magnitude for the mass and volume of MPs, as detailed in Kirstein et al., 2021. MP
188 concentrations were extrapolated to the initial sampling volumes. Because the number of
189 samples remained small, non-parametric statistics were used in the analysis.
190 Several precautions were applied to mitigate contamination. Glass vessels and filters were
191 all heated to 500°C for 2 h before use. All solutions used were filtered on GF/D Whatman
192 glass fibre filters (Sigma Aldrich, porosity: 2.7 µm). The vessels were rinsed with filtered
193 water and filtered using 50% ethanol. Laboratory coats of 100% cotton were worn and
194 plastic materials were avoided. The samples were stored in glass bottles. Glass bottles and
195 all beakers were covered with aluminium foil. The samples were sieved using a laminar flow
196 cabinet. Contamination during the different extraction steps was evaluated using procedural
197 blanks (n=10), which underwent the same steps as the samples.

198 ## 3. Results and discussion

199 ### 3.1. Microfiber and microplastic concentrations

200 During the flood event, MF concentrations ranged between 1.3 and 3.7 items/L, whereas MP
201 concentrations ranged from 10.4 to 34.4 items/L (Figure 3). In low flow conditions, MF
202 concentrations ranged from 1.9 to 5.5 items/L, whereas MP concentrations ranged from 9.3
203 to 26.5 items/L (min–max values). Median MF contamination was 0.3 items/L with an
204 interquartile range of 0.2 (n=10) whereas median MP contamination was 0.2 items/L with an
205 interquartile range of 0.2 (Figure 3).

206 Variations in the minimum and maximum concentrations of all samples were calculated for
207 each sampling site, under low flow conditions and during the flood (variation in concentration

= (Max-Min)/Min) * 100) (Table 1). Upstream and Downstream 1 presented relatively low variations between the minimum and maximum concentrations for both MFs (< 25%) and MPs (<71%) (Table 1). Downstream 2 presented the highest MF (229.8%) and MP concentrations (318.0%) (Figure 3) and the highest variability between minimum and maximum values (Table 1).

Table 1: Variation in concentrations between minimum and maximum values for each sampling site, for samples collected in low flow conditions and during the flood

	%Variation between min-max values for **MFs**	%Variation between min-max values for **MPs**
Upstream	14.4	49.0
Downstream 1	23.3	70.3
Downstream 2	318.0	229.8

If all samples are combined, we obtain MF and MP median concentrations of 2.6 and 15.5 items/L and interquartile ranges of 1.6 and 4.9 items/L, respectively (n = 10). Other studies in freshwater environments generally have found concentrations below 1 items/L (de Carvalho et al., 2021; Kataoka et al., 2019; Wong et al., 2020). The concentrations we found are comparable to those found in Cooks River, Australia (between 0.4 and 17.4 items/L, Hitchcock, 2020) and in the Maozhou River, China (between 3.5 and 25.5 items/L, Wu et al., 2020). We found that MPs were more abundant than MFs. Several studies have also reported fewer fibers than other shapes in freshwater samples (Mani and Burkhardt-Holm, 2020; Mao et al., 2020; Wu et al., 2020). Stereomicroscope counting did not enable the detection of MFs below 50 µm. Therefore, we may have underestimated the MF concentration. Despite a strong urban gradient and high water flow variability between sampling sites, MF and MP concentrations during low flow conditions have the same order of magnitude as the concentrations estimated during the flood event of January-February

2018 (Figure 3 and Table 1). Downstream 2 presented the highest variability (Table 1) and the highest concentrations (Figure 3) of MPs and MFs, both during low-flow conditions and the flood event. This may indicate a significant release of MPs related to WWTPs. However, Downstream 2 is located downstream the confluence with the Oise River (Figure 1), which was also flooded. This tributary is less urbanised and may dilute the microlitter inputs at this sampling site. However, the flood event did not significantly change the concentrations observed at the different sampling sites. As previously noted, contradictory results were found regarding the influence of water levels and flows on MP concentrations. The dilution of MPs during flood events has been reported in several studies (Rodrigues et al., 2018; Watkins et al., 2019; Wu et al., 2020), but does not seem to occur in the Seine River. Recent studies have shown that stormwater runoff could be a significant source of macroplastics (Treilles et al., 2021b) and microplastics during rain events (C. Liu et al., 2019; Treilles et al., 2021a). Precipitation may increase microlitter inputs through stormwater runoff. The increase in the flowrate during a flood implies remobilisation of the sediments owing to an increase in the shear strength, as well as remobilisation of MF and MP stored in sediments (Hurley et al., 2018). However, in the Seine River, waterway traffic may greatly influence this distribution. In 2019, 23.7 millions of tons of goods were transported by waterway traffic in the Seine River basin (Voies Navigables de France, 2020). This intense activity influences the sediment dynamics, which are not in a steady state (Vilmin, 2014). Waterway traffic intensively remobilises sediments even under low-flow conditions. This could partially explain the similar values observed between the flood and low-flow conditions. To ensure better comparability between studies, waterway traffic and sediment dynamics in a study area should be precisely recorded. The concentrations found in the Seine River are very high compared to those presented in a previous study on this river (~$3x10^{-4}$ MPs/L ; Dris et al., 2015). The Seine River concentrations are also high compared to those found in the Rhine (~ 1 × 10–3MPs/L ; Mani et al., 2015). Contrary to Wong et al. (2020), we found no statistically significant correlations between precipitation and concentration (Spearman's rs test, $p = 0.89$).

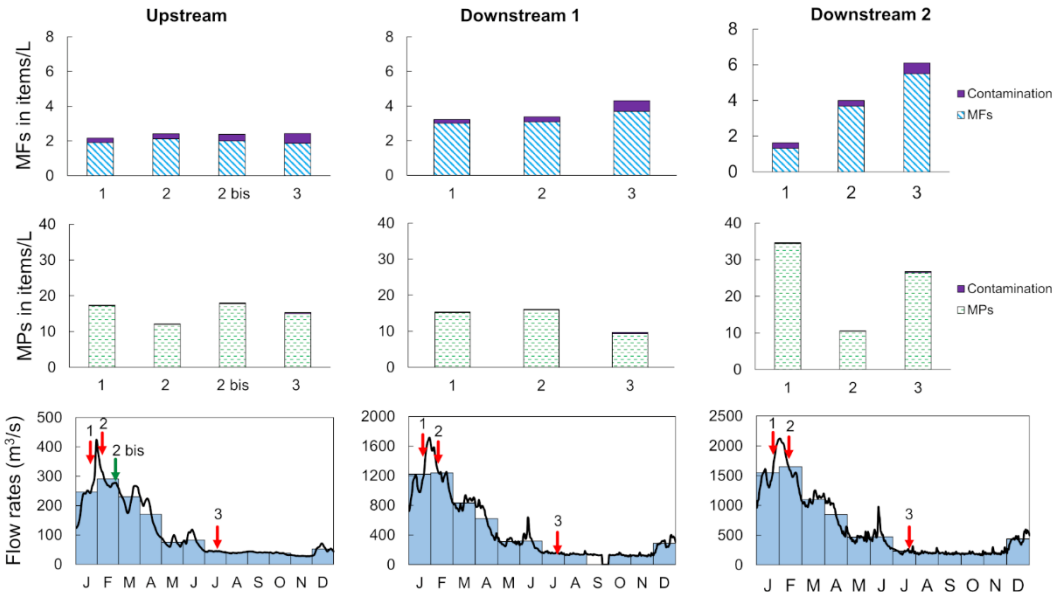

Figure 3: Microfiber and microplastic concentrations in the Seine river, relative to the hydrograph of each site (y-axis are different depending on the sampling site)

Regarding the spatial variations, concentrations between the upstream and downstream areas were of the same order of magnitude. This is consistent with previous data collected by Dris et al. (2018), who did not notice a significant impact of the urban gradient or variations in the flow rate on the MF or MP concentrations in the Seine River. These observations were confirmed by the present study at a larger scale. Based on the size and shape of the particles, the siMPle analysis software enables MP mass concentration estimates. However, it was not possible to estimate the mass of the MFs that we counted using a stereomicroscope. The order of magnitude for MP mass concentrations was comparable between the low flow period and the flood event, as shown in Table 2. We did not observe a significant concentration gradient between the upstream and downstream sites of Greater Paris in terms of mass concentrations, which is consistent with the results of Dris et al. (2018). In addition, Downstream 2 presented the highest mass concentrations in number of particles (Table 2). MP mass concentrations in freshwater environments have been only rarely estimated. Using the total weight/number of microplastics and non-metric multidimensional scaling (nMDS), Rodrigues et al., 2018 reported mass concentrations between 5 and 51.7 µg/L in Antuã River, Portugal. These values were comparable to our

276 estimations. Several studies have reported lower mass concentrations. In surface water
277 samples, Haberstroh et al. (2021) found a mean mass concentration of 5.4 µg/L in the
278 Hillsborough River, USA. Kataoka et al. (2019) observed variable MP mass concentrations
279 between 0 and 3.2 µg/L.

280 Table 2: Estimation of MP mass concentrations in Seine River water based on siMPle
281 software analysis.

	Median mass concentration during low flow period (µg/L)	Median mass concentration during the flood event (µg/L)
Upstream	10	20
Downstream 1	5	10
Downstream 2	80	50

282

283 3.2. Microfiber and microplastic size distribution

284 Boxplots of the MF and MP sizes relative to river discharge are shown in Figure 4. The size
285 distribution of these particles under low-flow conditions and during the flood event is
286 presented in Figure 5. During the flood event, the median MF sizes of Upstream,
287 Downstream 1, and Downstream 2 samples ranged from 1960 to 5410 µm, whereas the
288 median MP sizes ranged from 115 to 205 µm (Figure 4). The MF size distribution showed
289 the presence of large MFs >5 mm (Figure 5).

290 In low-flow conditions, the median MF sizes of Upstream, Downstream 1, and Downstream 2
291 samples ranged from 2500 to 3480 µm, whereas the median MP size ranged from 96 to 248
292 µm (Figure 4). As for the flood event, the MF size distribution showed the presence of large
293 MFs >5 mm (Figure 5). In contrast, the median MP size was below 250 µm. The MF and MP
294 size distributions during the flood and low-flow conditions are detailed in the supplementary
295 data (Table S2 and Table S3). The mean values were always higher than the median values
296 owing to the presence of large particles (> 5 mm for MFs and > 1 mm for MPs) (Figure 4).

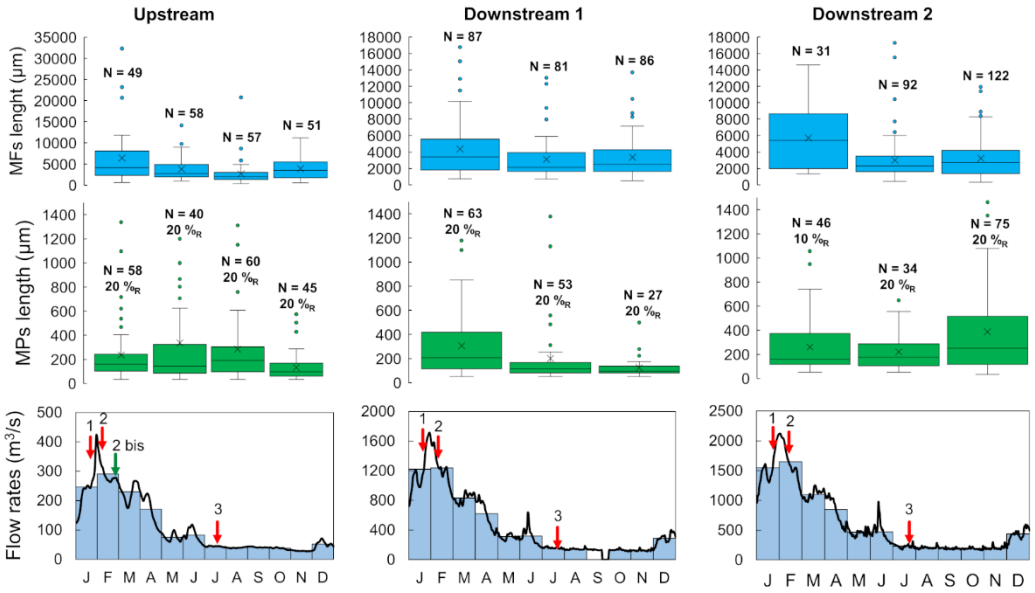

297

298 Figure 4: Boxplots of microfiber and microplastic length relative to the hydrographs of each
299 sampling site (y-axis may be different depending on the sampling site); mean values are
300 displayed as crosses; $\%_R$: resuspension percentage; N: number of particles

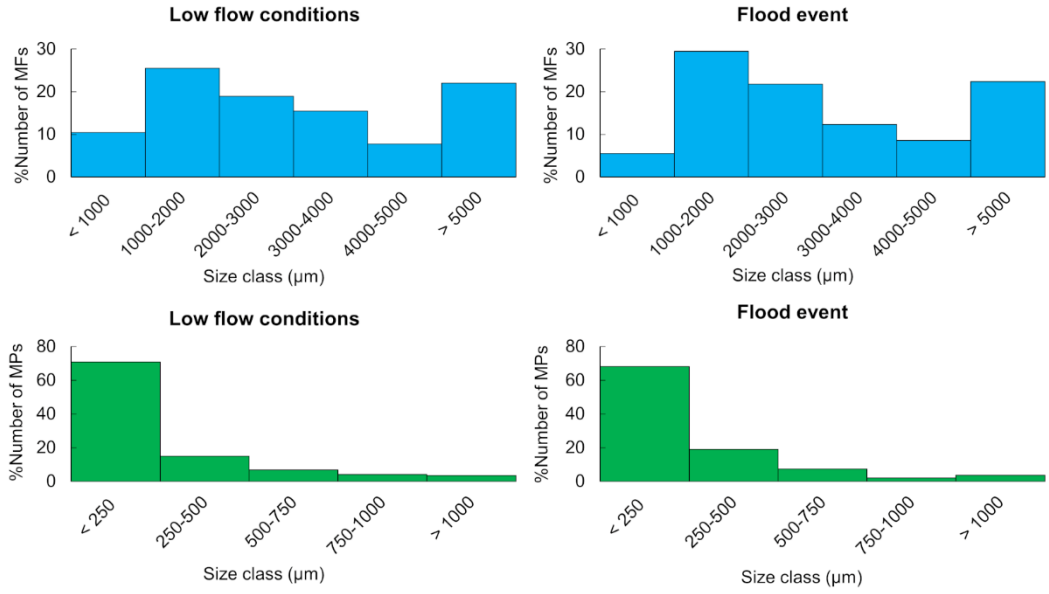

301

302 Figure 5: Microfiber and microplastic size distributions in low flow conditions and during the
303 flood event

304 According to Figure 5, the size distributions in low-flow conditions and during the flood event
305 are similar. MFs sizes were not significantly different between times of low river discharge
306 and floods, according to the Mann-Whitney test (n=259 in low flow conditions and n=455

during the flood; p = 0.33). The same trend was observed for MPs (MW test, n=147 in low-flow conditions and n=354 during the flood; p = 0.09). MFs and MPs found in the analytical blanks were significantly smaller than the particles analysed in the samples (MW test, p <0.05). The median number of MF and MP found in each analytical blank was 9 and 4, respectively, with a median size of 1800 µm and 104 µm, respectively (n=10).

More than 20% of MFs belonged to the > 5 mm size class (Figure 5). The minimum and maximum MF sizes of all the samples were 313 and 32328 µm, respectively. Even though more than 60% of MFs are smaller than 4 mm, the <1 mm size class is not the most abundant, in contrast with the size distribution of MFs found in atmospheric fallout (Allen et al., 2019). This size distribution differs from that found in a previous study on the Seine River, for which >1 mm was the most significant fraction (Dris et al., 2018).

More than 60% of MPs were smaller than 250 µm (Figure 5). This shows the importance of using a small mesh size for MP sampling. A 300 µm net may be inefficient in collecting the most significant MP size classes. The minimum and maximum MP sizes of all samples combined were 32 µm and 2 528 µm, respectively. When all samples were combined (for low flow periods and during the flood), 20% of all MPs were smaller than 80 µm. This may indicate that: (i) the 80 µm net clogged and stored small MPs or (ii) MP aggregates with various MP sizes could have accumulated in the net and could have been separated during organic matter digestion.

3.3. Polymer distribution

Polypropylene (PP) is the most common polymer (56–90%), followed by polyethylene (PE, 3–19%) and polyester (PES, 0–26%) in all samples (Figure 6). The category “other” from Figure 6 contains seven polymers, as detailed in the supplementary data (Table S4). For all samples, PP was always the most abundant polymer. PP and PE are commonly used in packaging, while PES is used in plastic bottles and textiles.

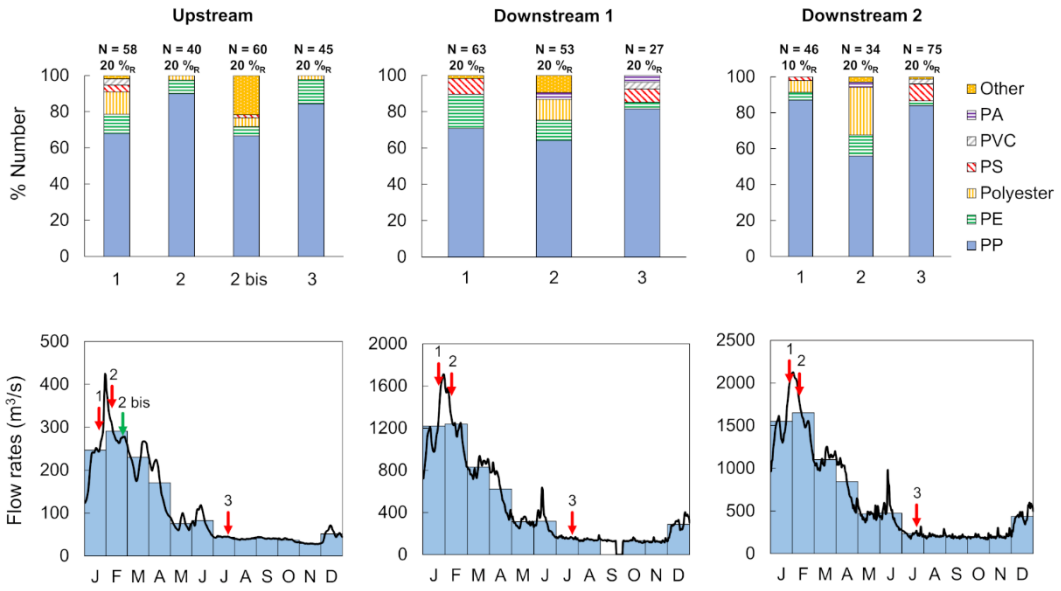

Figure 6: Percentage of polymers in each sample relative to river discharge at each site. N: number of microplastics (MP) particles found for a given resuspension volume; $\%_R$: resuspension percentage. PP: polypropylene; PE: polyethylene; PS: polystyrene; PVC: polyvinyl chloride; PA: polyamide;

The results do not show significant differences in polymer distributions between low flow conditions and the flood event (Figure 4-6, Table S4). The most significant polymers found in our samples (PP, PE, PES) are the same as the most representative polymers of macroplastic debris found in rivers (van Emmerik et al., 2018). These macroplastics may have formed MPs through fragmentation, which could explain the similarity in the polymer nature between these studies. The flood event had no significant impact on the type of polymer transported.

3.4. MPs and MFs fluxes in the Seine river

These similarities between low flow conditions and floods have strong implications for MF and MP fluxes in the Seine River. Considering the daily flowrates of each sampling site (assessed using Pont-sur-Seine, Austerlitz, and Vernon measurements, respectively; see Figure 2) and the MF and MP concentrations (first and third quartiles, see supplementary data Table S6), we calculated the MF and MP fluxes as the number of particles flowing per

year in the Seine River. We assumed that the MF and MP distributions were the same over the water column. For both MF and MP fluxes, we observed an increasing gradient from Upstream to Downstream 2 (Table 3).

The MF flux ranges from $6.6x10^{12}$ to $9.1x10^{13}$ items/year, increasing from Upstream to Downstream 2 (Table 3). Dris et al. (2018) previously estimated an anthropogenic MF flux in the Seine River between 2.8×10^{10} and $6.1x10^{11}$ particles/year. With the hypothesis that 65% of the MFs are synthetic, they approximated a flux between 1.8×10^{10} and 4.0×10^{11} of synthetic MFs per year. Owing to a lack of data, Dris et al. (2018) considered only fibers and not the fragments. We estimated much higher fluxes for anthropogenic MF fluxes. This difference may be linked to methodological differences between our studies. Samples from Dris et al. (2018) were collected with an 80 µm net plunged into the Seine River, while we pre-filtered raw water with an 80 µm net. This sampling difference may affect the concentrations observed in samples, as reported by Zheng et al. (2021), who found a difference in concentration of two orders of magnitude between the pre-filtration method and trawl net for the same sampling site.

For MPs, we calculated a flux between 4.9×10^{13} and 6.2×10^{14} items/year, increasing from Upstream to Downstream 2. µFTIR analyses coupled with the analysis software siMPle gave an order of magnitude for MP mass fluxes transported at each sampling site (Table 3). MP mass fluxes ranged between 58 and 1675 tonnes/year and increased from Upstream to Downstream 2. The MP mass fluxes at Downstream 2 are extremely high. The highest MP concentrations (Figure 3, Table 2 and Table S6) and highest flowrates were reported at this site, which explains the reported mass fluxes. As reported for the number of particles, Downstream 2 mass fluxes may be significant due to the different WWTP effluents (Figure 1). These significant mass fluxes may indicate high MP loads derived from urban water from the Paris megacity. Thus, MP mass fluxes are impacted by urbanisation.

375 Table 3: Estimations of MF and MP fluxes for each sampling point

	MF Fluxes in items/year	**MPs Fluxes in items/year**	**MPs Fluxes in tonnes/year**
Upstream	6.6-7.1x10^{12}	4.9-6.0x10^{13}	58-74
Downstream 1	4.4-4.8x10^{13}	1.8-2.2x10^{14}	56-146
Downstream 2	4.9-9.1x10^{13}	3.6-6.0x10^{14}	924-1675

376

377 The January-February 2018 flood event corresponded to 14.5% of the year (in time) but
378 contributed 40% of the microplastic and microfiber annual loads, indicating the important role
379 of flood events as microplastic inputs in the Seine River. This is consistent with the data
380 collected by Wagner et al. (2019), who found that 90% of the plastic load in freshwater could
381 be transported in 20% of the year. According to our results, we observed a significant
382 increase in MP mass fluxes from upstream to downstream sites, mainly caused by the
383 increase in flow rates and not by a significant concentration increase. For this reason, high
384 water levels may significantly increase the plastic load in freshwater. For macroplastic fluxes,
385 van Emmerik et al. (2019) observed an increase of one order of magnitude during high water
386 levels in the Seine River. According to Tramoy et al. (2020a), flood events may effectively
387 flush plastic debris from upstream to downstream regions owing to their high flow rates.

388 Tramoy et al. (2021, under review) estimated that the macroplastic mass fluxes from the
389 Seine River estuary to the ocean range between 100 and 200 metric tons per year. The high
390 value found in Downstream 2 is most likely linked to the significant mass concentrations and
391 high flowrates for this sampling point. Although MP mass concentrations are rarely assessed
392 in freshwater systems, our results are consistent with the estimations from Rodrigues et al.
393 (2018), but are one or two orders of magnitude higher than other estimations (Haberstroh et
394 al., 2021; Kataoka et al., 2019). These estimations may indicate significant plastic inputs
395 from the Greater Paris region. However, our estimation does not correspond to MP mass

discharge from land to sea, but only reflects the MP mass flux at certain sampling points. More data should be collected on plastic mass fluxes, particularly in urban rivers, to confirm the significant microplastic loads we observed.

4. Conclusion

We evaluated the MF and MP concentrations at three different upstream to downstream sampling sites during both low-flow conditions and a flood event. The results of this study show that the concentrations are of the same order of magnitude regardless of the hydrological conditions. The urbanisation gradient did not significantly influence these concentrations. Similarly, the flood and urbanisation gradient did not significantly affect the size and polymer distributions at the different sampling sites. PP, PE, and PES correspond to more than 60% of all polymers found. However, MP mass fluxes are strongly impacted by the urbanisation gradient, as we observed very high mass fluxes at the most downstream sampling site (924-1675 tonnes/year at Downstream 2). The January-February 2018 flood event, which corresponds to 14.5% of the year (in terms of time), contributed 40% of the MF and MP loads in the Seine River. In the future, greater attention should be paid to flood events, as they constitute major pathways for microlitter contamination. A better understanding of MF and MP dynamics in freshwater environments is needed to evaluate the impact of transitory events such as floods and significant rainfall events.

5. Acknowledgements

We would like to thank the Urban Pollutants Observatory (OPUR) project for its support and the OSU-Efluve for access to the µFTIR. We would also like to thank Mathilde Ropiquet and Léa Parent for their contributions to the sampling campaigns and microfiber counts during their internships.

References

Allen, S., Allen, D., Phoenix, V.R., Le Roux, G., Durántez Jiménez, P., Simonneau, A., Binet, S., Galop, D., 2019. Atmospheric transport and deposition of microplastics in a remote mountain catchment. Nat. Geosci. 12, 339–344. https://doi.org/10.1038/s41561-019-0335-5

Blettler, M.C.M., Ulla, M.A., Rabuffetti, A.P., Garello, N., 2017. Plastic pollution in freshwater ecosystems: macro-, meso-, and microplastic debris in a floodplain lake. Environ. Monit. Assess. 189, 581. https://doi.org/10.1007/s10661-017-6305-8

Cole, M., Lindeque, P., Halsband, C., Galloway, T.S., 2011. Microplastics as contaminants in the marine environment: A review. Mar. Pollut. Bull. 62, 2588–2597. https://doi.org/10.1016/j.marpolbul.2011.09.025

de Carvalho, A.R., Garcia, F., Riem-Galliano, L., Tudesque, L., Albignac, M., ter Halle, A., Cucherousset, J., 2021. Urbanization and hydrological conditions drive the spatial and temporal variability of microplastic pollution in the Garonne River. Sci. Total Environ. 769. https://doi.org/10.1016/j.scitotenv.2020.144479

Dris, R., Gasperi, J., Mirande, C., Mandin, C., Guerrouache, M., Langlois, V., Tassin, B., 2017. A first overview of textile fibers, including microplastics, in indoor and outdoor environments. Environ. Pollut. 221, 453–458. https://doi.org/10.1016/j.envpol.2016.12.013

Dris, R., Gasperi, J., Rocher, V., Saad, M., Renault, N., Tassin, B., 2015. Microplastic contamination in an urban area: a case study in Greater Paris. Environ. Chem. 12, 592–599. https://doi.org/10.1071/EN14167

Dris, R., Gasperi, J., Tassin, B., 2018. Sources and Fate of Microplastics in Urban Areas: A Focus on Paris Megacity. Freshw. Microplastics 69–83. https://doi.org/10.1007/978-3-319-61615-5_4

Gall, S.C., Thompson, R.C., 2015. The impact of debris on marine life. Mar. Pollut. Bull. 92, 170–179. https://doi.org/10.1016/j.marpolbul.2014.12.041

Haberstroh, C.J., Arias, M.E., Yin, Z., Wang, M.C., 2021. Effects of hydrodynamics on the cross-sectional distribution and transport of plastic in an urban coastal river. Water Environ. Res. 93, 186–200. https://doi.org/10.1002/wer.1386

Hitchcock, J.N., 2020. Storm events as key moments of microplastic contamination in aquatic ecosystems. Sci. Total Environ. 734, 139436. https://doi.org/10.1016/j.scitotenv.2020.139436

Horton, A.A., Walton, A., Spurgeon, D.J., Lahive, E., Svendsen, C., 2017. Microplastics in freshwater and terrestrial environments: Evaluating the current understanding to identify the knowledge gaps and future research priorities. Sci. Total Environ. 586, 127–141. https://doi.org/10.1016/j.scitotenv.2017.01.190

Hurley, R., Woodward, J., Rothwell, J., 2018. Microplastic contamination of river beds significantly reduced by catchment-wide flooding. Nat. Geosci. https://doi.org/10.1038/s41561-018-0080-1

Jamieson A. J., Brooks L. S. R., Reid W. D. K., Piertney S. B., Narayanaswamy B. E., Linley T. D., 2019. Microplastics and synthetic particles ingested by deep-sea amphipods in six of the deepest marine ecosystems on Earth. R. Soc. Open Sci. 6, 180667. https://doi.org/10.1098/rsos.180667

Kataoka, T., Nihei, Y., Kudou, K., Hinata, H., 2019. Assessment of the sources and inflow processes of microplastics in the river environments of Japan. Environ. Pollut. 244, 958–965. https://doi.org/10.1016/j.envpol.2018.10.111

Kirstein, I.V., Hensel, F., Gomiero, A., Iordachescu, L., Vianello, A., Wittgren, H.B., Vollertsen, J., 2021. Drinking plastics? – Quantification and qualification of microplastics in drinking water distribution systems by µFTIR and Py-GCMS. Water Res. 188, 116519. https://doi.org/10.1016/j.watres.2020.116519

Klein, S., Worch, E., Knepper, T.P., 2015. Occurrence and Spatial Distribution of Microplastics in River Shore Sediments of the Rhine-Main Area in Germany. Environ. Sci. Technol. 49, 6070–6076. https://doi.org/10.1021/acs.est.5b00492

Liu, C., Li, J., Zhang, Y., Wang, L., Deng, J., Gao, Y., Yu, L., Zhang, J., Sun, H., 2019. Widespread distribution of PET and PC microplastics in dust in urban China and their estimated human exposure. Environ. Int. 128, 116–124. https://doi.org/10.1016/j.envint.2019.04.024

Liu, F., Olesen, K.B., Borregaard, A.R., Vollertsen, J., 2019. Microplastics in urban and highway stormwater retention ponds. Sci. Total Environ. 671, 992–1000. https://doi.org/10.1016/j.scitotenv.2019.03.416

Mani, T., Burkhardt-Holm, P., 2020. Seasonal microplastics variation in nival and pluvial stretches of the Rhine River – From the Swiss catchment towards the North Sea. Sci. Total Environ. 707, 135579. https://doi.org/10.1016/j.scitotenv.2019.135579

Mani, T., Hauk, A., Walter, U., Burkhardt-Holm, P., 2015. Microplastics profile along the Rhine River. Sci. Rep. 5, 17988. https://doi.org/10.1038/srep17988

Mao, Y., Li, H., Gu, W., Yang, G., Liu, Y., He, Q., 2020. Distribution and characteristics of microplastics in the Yulin River, China: Role of environmental and spatial factors. Environ. Pollut. 265, 115033. https://doi.org/10.1016/j.envpol.2020.115033

Rodrigues, M.O., Abrantes, N., Gonçalves, F.J.M., Nogueira, H., Marques, J.C., Gonçalves, A.M.M., 2018. Spatial and temporal distribution of microplastics in water and sediments of a freshwater system (Antuã River, Portugal). Sci. Total Environ. 633, 1549–1559. https://doi.org/10.1016/j.scitotenv.2018.03.233

Roebroek, C.T.J., Harrigan, S., Emmerik, T.H.M. van, Baugh, C., Eilander, D., Prudhomme, C., Pappenberger, F., 2021. Plastic in global rivers: are floods making it worse? Environ. Res. Lett. 16, 025003. https://doi.org/10.1088/1748-9326/abd5df

Schmidt, L.K., Bochow, M., Imhof, H.K., Oswald, S.E., 2018. Multi-temporal surveys for microplastic particles enabled by a novel and fast application of SWIR imaging spectroscopy – Study of an urban watercourse traversing the city of Berlin, Germany. Environ. Pollut. 239, 579–589. https://doi.org/10.1016/j.envpol.2018.03.097

Tramoy, R., Gasperi, J., Colasse, L., Silvestre, M., Dubois, P., Noûs, C., Tassin, B., 2020a. Transfer dynamics of macroplastics in estuaries – New insights from the Seine estuary: Part 2. Short-term dynamics based on GPS-trackers. Mar. Pollut. Bull. 160, 111566. https://doi.org/10.1016/j.marpolbul.2020.111566

Tramoy, R., Gasperi, J., Colasse, L., Tassin, B., 2020b. Transfer dynamic of macroplastics in estuaries — New insights from the Seine estuary: Part 1. Long term dynamic based on date-prints on stranded debris. Mar. Pollut. Bull. 152, 110894. https://doi.org/10.1016/j.marpolbul.2020.110894

Treilles, R., Cayla, A., Gaspéri, J., Strich, B., Ausset, P., Tassin, B., 2020. Impacts of organic matter digestion protocols on synthetic, artificial and natural raw fibers. Sci. Total Environ. 748, 141230. https://doi.org/10.1016/j.scitotenv.2020.141230

Treilles, R., Gasperi, J., Gallard, A., Saad, M., Dris, R., Partibane, C., Breton, J., Tassin, B., 2021a. Microplastics and microfibers in urban runoff from a suburban catchment of Greater Paris. Sci. Total Environ.

Treilles, R., Gasperi, J., Saad, M., Tramoy, R., Breton, J., Rabier, A., Tassin, B., 2021b. Abundance, composition and fluxes of plastic debris and other macrolitter in urban runoff in a suburban catchment of Greater Paris. Water Res. 192, 116847. https://doi.org/10.1016/j.watres.2021.116847

van Emmerik, T., Kieu-Le, T.-C., Loozen, M., Oeveren, K., Strady, E., Bui, X.-T., Egger, M., Gasperi, J., Lebreton, L., Nguyen, P.-D., Schwarz, A., Slat, B., Tassin, B., 2018. A methodology to characterize riverine macroplastic emission into the ocean. Front. Mar. Sci. 5. https://doi.org/10.3389/fmars.2018.00372

van Emmerik, T., Tramoy, R., van Calcar, C., Alligant, S., Treilles, R., Tassin, B., Gasperi, J., 2019. Seine Plastic Debris Transport Tenfolded During Increased River Discharge. Front. Mar. Sci. 6. https://doi.org/10.3389/fmars.2019.00642

524 Veerasingam, S., Mugilarasan, M., Venkatachalapathy, R., Vethamony, P., 2016. Influence
525 of 2015 flood on the distribution and occurrence of microplastic pellets along the
526 Chennai coast, India. Mar. Pollut. Bull. 109, 196–204.
527 https://doi.org/10.1016/j.marpolbul.2016.05.082
528 Vilmin, L., 2014. Modélisation du fonctionnement biogéochimique de la Seine de
529 l'agglomération parisienne à l'estuaire à différentes échelles temporelles (phdthesis).
530 Ecole Nationale Supérieure des Mines de Paris.
531 Voies Navigables de France, 2020. Transport et tourisme fluvial : les chiffres clés 2019.
532 Wagner, S., Klöckner, P., Stier, B., Römer, M., Seiwert, B., Reemtsma, T., Schmidt, C.,
533 2019. Relationship between Discharge and River Plastic Concentrations in a Rural
534 and an Urban Catchment. Environ. Sci. Technol. 53, 10082–10091.
535 https://doi.org/10.1021/acs.est.9b03048
536 Watkins, L., Sullivan, P.J., Walter, M.T., 2019. A case study investigating temporal factors
537 that influence microplastic concentration in streams under different treatment
538 regimes. Environ. Sci. Pollut. Res. Int. https://doi.org/10.1007/s11356-019-04663-8
539 Witzig, C.S., Földi, C., Wörle, K., Habermehl, P., Pittroff, M., Müller, Y.K., Lauschke, T.,
540 Fiener, P., Dierkes, G., Freier, K.P., Zumbülte, N., 2020. When Good Intentions Go
541 Bad—False Positive Microplastic Detection Caused by Disposable Gloves. Environ.
542 Sci. Technol. 54, 12164–12172. https://doi.org/10.1021/acs.est.0c03742
543 Wong, G., Löwemark, L., Kunz, A., 2020. Microplastic pollution of the Tamsui River and its
544 tributaries in northern Taiwan: Spatial heterogeneity and correlation with
545 precipitation. Environ. Pollut. 260, 113935.
546 https://doi.org/10.1016/j.envpol.2020.113935
547 Wu, P., Tang, Y., Dang, M., Wang, S., Jin, H., Liu, Y., Jing, H., Zheng, C., Yi, S., Cai, Z.,
548 2020. Spatial-temporal distribution of microplastics in surface water and sediments of
549 Maozhou River within Guangdong-Hong Kong-Macao Greater Bay Area. Sci. Total
550 Environ. 717, 135187. https://doi.org/10.1016/j.scitotenv.2019.135187
551 Zhao, S., Zhu, L., Li, D., 2016. Microscopic anthropogenic litter in terrestrial birds from
552 Shanghai, China: Not only plastics but also natural fibers. Sci. Total Environ. 550,
553 1110–1115. https://doi.org/10.1016/j.scitotenv.2016.01.112
554 Zheng, Y., Li, J., Sun, C., Cao, W., Wang, M., Jiang, F., Ju, P., 2021. Comparative study of
555 three sampling methods for microplastics analysis in seawater. Sci. Total Environ.
556 765, 144495. https://doi.org/10.1016/j.scitotenv.2020.144495
557

Supplementary data

Table S1: Daily flowrates, water levels and sampling volumes corresponding to each sample (data from http://hydro.eaufrance.fr)

			Upstream	Downstream 1	Downstream 2
1	01/26/2018	Flowrates (m^3/s)	280	1570	1880
		Water level (m)	6.19	5.49	3.39
		Sampling volume (L)	23	27	19
2	02/05/2018	Flowrates (m^3/s)	330	1460	1940
		Water level (m)	6.28	5.28	5.03
		Sampling volume (L)	24	24	23
2bis	02/21/2018	Flowrates (m^3/s)	256	-	-
		Water level (m)	6.19	-	-
		Sampling volume (L)	24	-	-
3	07/17/2018	Flowrates (m^3/s)	45	155	241
		Water level (m)	4.01	0.97	3.36
		Sampling volume (L)	21	20	20

Table S2: Summary of microfibers and microplastics sizes collected during a flood event

Microfibers	**N**	**Mean (µm)**	**Standard deviation (µm)**	**Median (µm)**	**Interquartile range (µm)**
Upstream	164	4153	4388	2716	3092
Downstream 1	168	3762	3036	2670	2983
Downstream 2	123	3699	3254	2453	2863

Microplastics	**N**	**Mean (µm)**	**Standard deviation (µm)**	**Median (µm)**	**Interquartile range (µm)**
Upstream	158	278	351	171	185
Downstream 1	116	258	255	150	215
Downstream 2	80	243	201	163	198

Table S3: Summary of microfibers and microplastics sizes collected during low flow conditions

Microfibers	**N**	**Mean (µm)**	**Standard deviation (µm)**	**Median (µm)**	**Interquartile range (µm)**
Upstream	51	3923	2705	3482	3536
Downstream 1	86	3363	2531	2512	2608
Downstream 2	122	3221	2337	2687	2675

Microplastics	N	Mean (µm)	Standard deviation (µm)	Median (µm)	Interquartile range (µm)
Upstream	45	133	116	96	90
Downstream 1	27	124	91	96	56
Downstream 2	75	386	409	249	390

Table S4: Details of the category “Other” from Figure 6

Polymers from the category "Other"	Abbreviation
Acrylonitrile butadiene styrene	ABS
Cellulose Acetate	CA
Polyacrylonitrile	PAN
Polyamide	PA
Polyurethane	PU
Polyvinyl Acetate	PVAC
Styrene butadiene rubber	SBR

Table S5 : Details of the polymers found in the different samples

	Number of polymer types found	Details
260118_Upstream	7	CA, PAN, PE, PES, PP, PS, PVC
260118_Downstream 1	5	ABS, PE, PP, PS, SBR
260118_Downstream 2	4	PE, PES, PP, PS
050218_Upstream	3	PE, PES, PP
050218_Downstream 1	5	PA, PE, PES, PP, PVAC
050218_Downstream 2	5	PA, PE, PES, PP, PU
210218_Upstream	6	PAN, PE, PES, PP, PS, PVAC
170718_Upstream	3	PE, PES, PP
170718_Downstream 1	5	PA, PE, PP, PS, PVC
170718_Downstream 2	5	ABS, PE, PP, PS, PVC

574 Table S6: MF and MP concentrations (first and third quartile) for each sampling site

	First and third quartile (concentration in microfibers per liter)	First and third quartile (concentration in microplastics per liter)	First and third quartile (concentration in µg of microplastics per liter)
Upstream	1.9-2.0	14.3-17.4	16.8-21.3
Downstream 1	3.0-3.4	12.3-15.6	3.9-10.3
Downstream 2	2.5-4.6	18.5-30.4	47.0-85.1

575